

Constraining the dark fluid

Martin Kunz,¹ Andrew R. Liddle,¹ David Parkinson,¹ and Changjun Gao²

¹*Astronomy Centre, University of Sussex, Brighton BN1 9QH, United Kingdom*

²*The National Astronomical Observatories, Chinese Academy of Sciences, Beijing, 100012, China*

(Dated: November 2, 2021)

Cosmological observations are normally fit under the assumption that the dark sector can be decomposed into dark matter and dark energy components. However, as long as the probes remain purely gravitational, there is no unique decomposition and observations can only constrain a single dark fluid; this is known as the dark degeneracy. We use observations to directly constrain this dark fluid in a model-independent way, demonstrating in particular that the data cannot be fit by a dark fluid with a single constant equation of state. Parameterizing the dark fluid equation of state by a variety of polynomials in the scale factor a , we use current kinematical data to constrain the parameters. While the simplest interpretation of the dark fluid remains that it is comprised of separate dark matter and cosmological constant contributions, our results cover other model types including unified dark energy/matter scenarios.

PACS numbers: 95.36.x, 98.80.-k

I. INTRODUCTION

The standard cosmological model appeals to two separate dark components — dark matter and dark energy — and the usual application of observational constraints places limits on each of these. However, at present these two components have only been detected through their gravitational influence, and these measurements do not provide enough information to permit a unique decomposition into these components. Rather, it is a model assumption that the two components are separate. This point was first made in Ref. [1] and specific consequences explored in Refs. [2, 3]. Ref. [4] extended it to coupled models and named it the dark degeneracy.

This degeneracy is extremely general. One can write

$$G_{\mu\nu} - \kappa T_{\mu\nu}^{\text{visible}} = \kappa T_{\mu\nu}^{\text{dark}} \quad (1)$$

where $G_{\mu\nu}$ is the Einstein tensor, $T_{\mu\nu}$ the energy-momentum tensor, and κ the gravitational coupling. Any gravitational probe of the dark sector amounts to evaluating the left-hand side of this equation, and interpreting the non-zero result as evidence for the dark sector. Having obtained the dark sector energy-momentum tensor this way, such observations can offer no guidance on how that tensor might be split amongst different dark components.¹

Although the degeneracy holds even for structure formation probes (both linear and non-linear) of the dark sector, we will focus here only on kinematical probes, i.e. those referring to the homogeneous and isotropic background cosmology. A complete dark sector description is

then given by the total dark sector energy density and its equation of state w_{dark} , the latter determining the evolution of the former. This enables a simple analysis. To include structure formation data, while retaining statistical homogeneity, one would also need to consider at least the dark sector sound speed and perhaps also anisotropic stress [1, 4], and one might expect that structure formation observations would end up mostly constraining their form rather than imposing further upon w_{dark} .

As a simple example [1], in the standard cosmological model the redshift evolution of the total dark sector equation of state

$$w_{\text{dark}} \equiv \frac{\sum \rho_i w_i}{\sum \rho_i}, \quad (2)$$

(where ‘ i ’ runs over the dark components) is given by

$$w_{\text{dark}}^{\text{SCM}}(z) = -\frac{1 - \Omega_{\text{m},0}}{1 - \Omega_{\text{m},0} + (\Omega_{\text{m},0} - \Omega_{\text{b},0})(1+z)^3}, \quad (3)$$

$$\simeq -\frac{1}{1 + 0.31(1+z)^3}. \quad (4)$$

Here Ω_{m} and Ω_{b} are the total matter density parameter and the baryon density parameter, and the subscript indicates present value. The second line follows from inserting the values $\Omega_{\text{m},0} \simeq 0.274$ and $\Omega_{\text{b},0} \simeq 0.046$ obtained from current data compilations [6].

Inclusion of a single dark energy component with this equation of state evolution would give the same observational predictions as the standard cosmology. Indeed, once one allows the dark energy equation of state to evolve arbitrarily, one cannot say anything from observations about the dark matter density Ω_{dm} , as its effects can always be reinterpreted as due to the dark energy. Analyses which appear to measure Ω_{dm} accurately only manage to do so because the dark energy parameterization adopted is not general enough to be able to mimic the form of Eq. (3).

¹ We work entirely in Einsteinian gravity. A somewhat related issue arises in modified gravity models, where the ‘non-Einsteinian’ gravitational terms could be shifted to the right-hand side of the generalized Einstein equation and potentially reinterpreted as matter terms, see e.g. Ref. [5].

This degeneracy is perfect. All we can say in a model-independent way is that the present total dark sector density is about 0.95, and that its equation of state is constrained to evolve in a particular way from an early-time value at or near zero to arrive at its present value of $w_{\text{dark}}^{\text{obs}}(z=0) \simeq -0.8$. Our aim in this paper is to more precisely quantify these constraints, by considering general dark sector models that do not include a pure cold dark matter component.

II. MODELS AND DATA

Having set up this non-standard framework for analyzing the dark sector, our analysis procedure is standard and straightforward.

A. Models

In order to impose constraints on the dark fluid, we need to employ a parameterization of its equation of state. Henceforth we drop the subscript ‘dark’, using w throughout as the total dark sector equation of state. As we wish to reach high redshift, we parameterize w as a function of scale factor a , which has the bounded domain $0 < a \leq 1$. We simply expand this as a power series in a at the present, which we find to be sufficient. At linear order this is the well-known CPL parameterization $w = w_0 + (1-a)w_1$ [7], normally applied to the dark energy alone but here referring to the combined dark sector. To general order this expression was given, again for the dark energy alone, in Ref. [8], which in actual calculation considered the linear and quadratic versions. As we are demanding that our parameterization describe the entire dark sector, we will explore up to cubic order. Our models are hence

$$w(a) = \sum_{n=0}^N w_n (1-a)^n \quad (5)$$

for different choices of N .

As we will see, the data strongly demand that $w(a)$ is close to zero as $a \rightarrow 0$, i.e. the dark sector is required to behave as dark matter at early times (note that this is true even without inclusion of any structure formation data). Accordingly we will also consider the same expansions supplemented with the additional constraint $w(a=0) = 0$ which fixes their highest-order term as a function of the others, and with the combined constraints $w(a=0) = 0$ and $dw/da|_{a=0} = 0$. We will call these the ‘constrained’ and ‘doubly-constrained’ expansions respectively. The former can be used from linear order upwards, and the latter from quadratic upwards.

In all cases we choose priors on the expansion coefficients which are wide enough that the outcome is determined entirely by the data and not the prior.

The standard rulers measured by the cosmic microwave background (CMB) and baryon acoustic oscillations (BAO) are all fixed by the sound horizon at decoupling (which we fix to be $z_{\text{dec}} = 1089$), which is dependent on the baryon density. The standard rulers are all distance ratios independent of H_0 , and the supernovae make no measurement of the Hubble parameter H_0 since it is degenerate with the unknown absolute normalization over which we marginalize. As our data compilation does not constrain H_0 , it is not able to give an accurate constraint on the total dark sector energy density. However the physical baryon density $\Omega_b h^2$ is accurately measured to the usual value, and so if supplemented with a direct determination of H_0 , we would find the expected total dark sector energy density $\Omega_{\text{dark}} \simeq 0.95$. In our analysis we allow $\Omega_b h^2$ and H_0 to vary, but constrain them using other datasets, and marginalize over them, in effect marginalizing over the total dark sector energy density.

In light of the above, when we quote model parameter counts they are of the dark sector equation of state, and do not include the total dark sector energy density. For the general dark sector models, we quote the number of parameters specifying $w(a)$. For Λ CDM, the equivalent parameter is the relative amount of dark matter and dark energy at present (equivalently, the coefficient of the $(1+z)^3$ term in Eq. (4)).

B. Data

We use a fairly typical combination of kinematical data to constrain our models. Standard candle data comes from supernova type Ia luminosity distances, for which we use the cut Union supernova sample [10] (with systematic errors included), and standard ruler data comes from the angular positions of the CMB [11] and BAO peaks [12]. Note that Ref. [11] give constraints on the scaled distance to recombination R and the angular scale of the sound horizon l_a . These are defined to be

$$R \equiv \sqrt{\Omega_m H_0^2} r(z_{\text{CMB}}), \quad l_a \equiv \frac{\pi r(z_{\text{CMB}})}{r_s(z_{\text{CMB}})}. \quad (6)$$

Since R is scaled by the physical matter density, and so makes assumptions about the separability of the dark matter and dark energy, we ignore it in this work. We use only the constraints on l_a , as well as those on $\Omega_b h^2$ and the correlations between the two. This still assumes that the sound speed of the dark component at high redshift is small, in order to avoid an early ISW effect shifting the peak position. We also include the SHOES (Supernovae and H_0 for the Equation of State) measurement of the Hubble parameter today, $H_0 = 74.2 \pm 3.6 \text{ kms}^{-1} \text{ Mpc}^{-1}$ [9].

TABLE I: Parameters (of the dark sector equation of state) and best-fit chi-squared for our various models. The constrained models force $w(a=0) = 0$, and the doubly-constrained ones additionally $dw/da|_{a=0} = 0$.

Model	Dark sector parameters	χ^2_{\min}
Λ CDM	1	311.9
Constant w	1	391.3
Linear (CPL)	2	312.1
Constrained linear	1	320.5
Quadratic	3	309.8
Constrained quadratic	2	311.9
Doubly-constrained quadratic	1	313.5
Cubic	4	309.6
Constrained cubic	3	311.1
Doubly-constrained cubic	2	311.5

III. RESULTS

Table I shows the number of adjustable parameters and best-fit chi-squared for most models, including Λ CDM for comparison. The total number of data points is 313 (308 SN-Ia, 2 BAO, 2 CMB and 1 from the SHOES project), but correlations between the data points make it difficult to state the number of independent data points, and so the number of degrees of freedom. We can say that the number of degrees of freedom is, at most, 311 minus the number of dark sector parameters, meaning that the data is an acceptable fit to all the models, except the constant w model, if the correlations are small.

The corresponding $w(a)$ curves of the best-fitting version of each model are shown in Fig. 1. The immediate conclusions from these are as follows:

1. Λ CDM, as expected, does a good job of fitting the data, bettered only by other models with more dark sector parameters. For our data the best-fit Ω_m is 0.26 ± 0.02 . This agrees well with the result of Komatsu et al. [6], with somewhat larger uncertainty as less data is being used.
2. Even the best-fit version of the constant w model is a very poor fit. The dark sector has not had a constant equation of state throughout its evolution.
3. The full four-parameter cubic does not significantly improve the fit over the three-parameter quadratic, indicating that three-parameter models saturate the constraining power of the data.
4. All the models have $w(a=0)$ at or very close to zero, enforced entirely by the data. This indicates that the full phenomenology can be captured using the constrained versions of the expansion, reducing the variable parameter set by at least one.
5. The doubly-constrained quadratic (i.e. simply $w(a) = w_0 a^2$) gives a tolerable one-parameter fit to

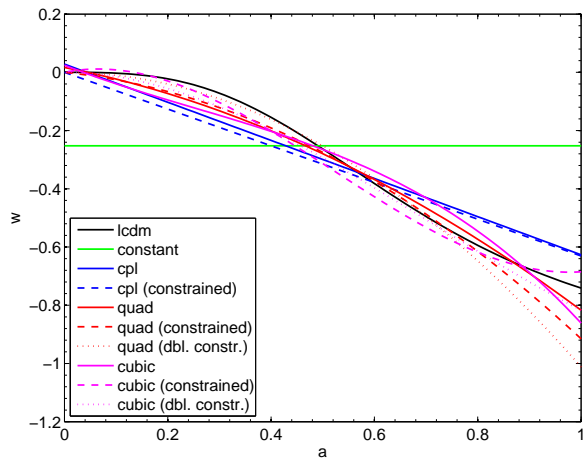


FIG. 1: The best-fit $w(a)$ for our various models. Note that the approach to $w = 0$ at $a = 0$ is determined entirely by the data in the unconstrained cases, while being enforced in the constrained models.

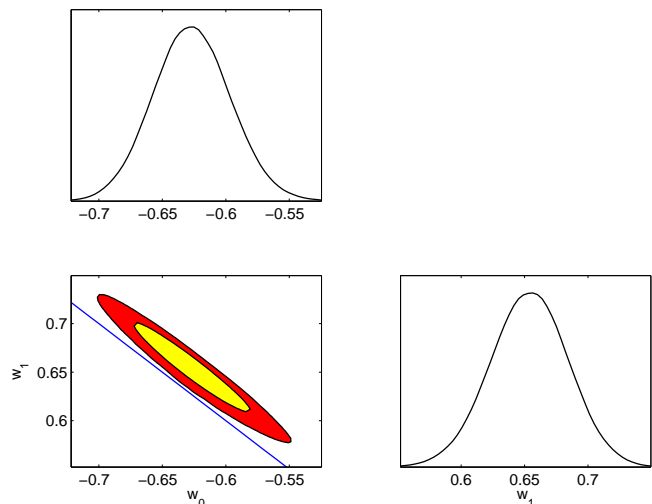


FIG. 2: Parameter constraints on the linear (CPL) parameterization. The constrained models lie on the line $w_1 = -w_0$, shown as the (blue) line on the w_0, w_1 plot.

the data, though not quite as good as the Λ CDM fit. By contrast, the single-parameter constrained linear fit is a poor fit to the data when compared to the Λ CDM fit which has the same number of parameters (though the general CPL model can acceptably fit it by overshooting to $w > 0$ at early times).

6. In terms of giving good fits to the data for economical numbers of parameters, apart from Λ CDM the two-parameter constrained quadratic and doubly-constrained cubic fits are the most appealing models.

More relevant than the best-fit parameters are the ranges of parameter values permitted by the data. As

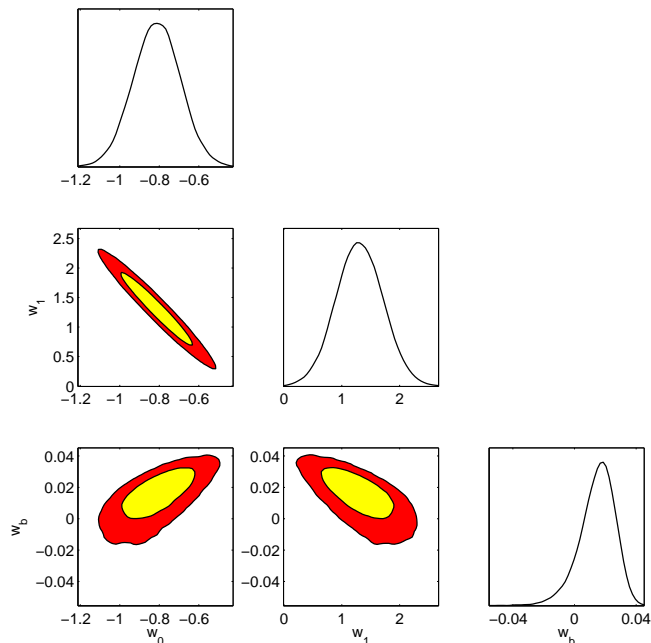


FIG. 3: Parameter constraints on the quadratic parameterization. Here $w_b = w_0 + w_1 + w_2$, which is the combination which is held at zero in the constrained quadratic case.

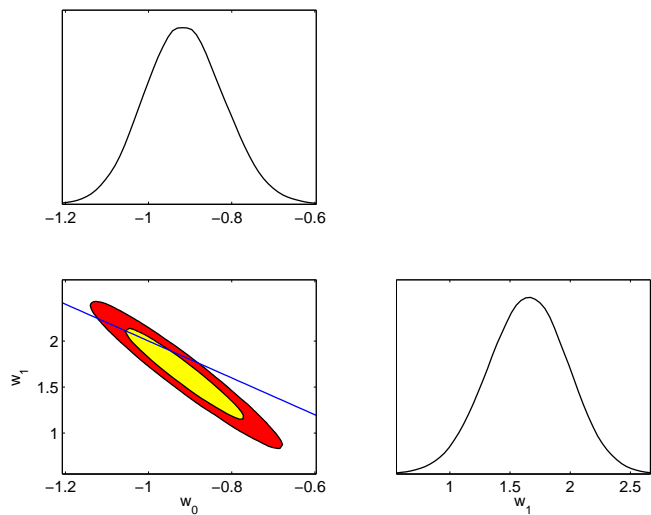


FIG. 4: Parameter constraints on the constrained quadratic parameterization, where $w(a=0)$ is set to zero. The doubly-constrained models lie on the line $w_1 = -2w_0$, shown as the (blue) line on the w_0, w_1 plot.

all constant w models are ruled out, we show in Figs. 2 and 3 the constraints on the parameters of the CPL and quadratic parameterizations, and in Fig. 4 we show the constraints on the constrained quadratic model, which forces $w(a=0) = 0$.

For illustrative purposes, Fig. 5 shows 400 quadratic $w(a)$ curves drawn randomly from the Markov chain. They are shaded so that the likelihood increases from

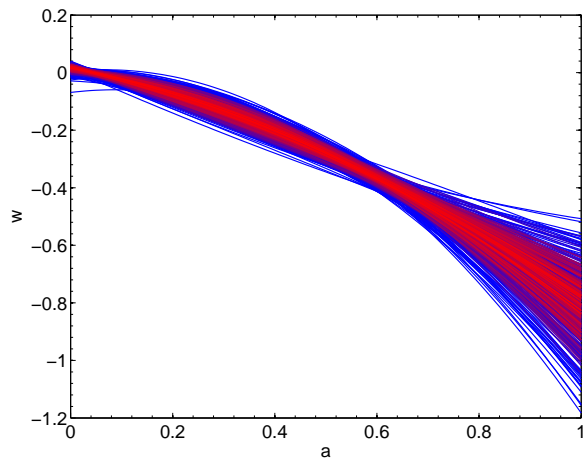


FIG. 5: An illustration of the form of the best fitting $w(a)$ curves for the quadratic case. A sparse sampling of 400 chain elements, colour coded by likelihood with the red (lighter) shading the highest, is shown.

blue (darker) to red (lighter). We can see that the high-redshift region near $a = 0$ is strongly constrained and requires $w \approx 0$, while the value of the total equation of state parameter today, $w_0 = w(a=1)$, is only very weakly constrained by the data sets used in this work.² Due to the integrated nature of the distance constraints on w , curves that oscillate around the best-fit incur only a small penalty. This becomes more problematic when going to higher order in power law expansions since then more oscillations become possible. As the oscillations have to average out, the expansion parameters are highly correlated and not really independent, which can already be seen for w_0 and w_1 in the quadratic case in Fig. 3.

We also carried out a different analysis where the equation of state w is allowed to take different values in binned regions of scale factor a , for simplicity taken to be linearly spaced with 10 or 20 bins. A Principal Component Analysis showed that three modes were well measured ($\sigma < 0.1$), supporting the conclusions above. This analysis also showed that the best measured mode was peaked in the highest-redshift bin.

IV. CONCLUSIONS

Due to the dark degeneracy, there is no unique split into dark matter and dark energy. For this reason, we considered in this paper the total dark sector equation of state. We parameterized it with polynomial expansions in the scale factor a and used type Ia supernovae, baryon

² As we were completing this work, Mortonson et al. [13] arXived a paper considering this specific point in much more detail. This point had also previously been noted in Ref. [14].

acoustic oscillations, and the CMB peak position to find constraints on the expansion parameters.

The strongest constraints come at very high redshift, from the CMB and BAO measurements of the sound horizon at decoupling. There the dark fluid must evolve with an equation of state close to zero, to recover the correct angular scale of the acoustic oscillations. At low redshift the constraints from SN-Ia and BAO are weaker, but require a negative pressure fluid with $w_{\text{dark}} \simeq -0.8$.

We found that Λ CDM gave the best one-parameter fit to current data, bettered only by other models with at least two parameters such as the doubly-constrained cubic expansion. However, none did very much better than Λ CDM. Accordingly, Λ CDM remains the most compelling interpretation of present data, despite the dark degeneracy. Nevertheless our polynomial fits indicate the constraints that can be applied to more general types of dark sector model.

One could speculate about how future measurements of the same general type might tighten our constraints, but as remarked in the introduction they cannot address the issue of separability of the dark sector into components. Rather, to defeat the dark degeneracy what is needed

are *non-gravitational* probes of the sector, for instance direct detection of dark matter particles at accelerators or in underground experiments [4]. Such detections would immediately move such particles from the dark sector to the ‘known’ sector, removing them from the dark sector degeneracy.

Acknowledgments

M.K., A.R.L., and D.P. were supported by STFC (UK). C.G. was supported by the National Science Foundation of China under the Distinguished Young Scholar Grant 10525314, the Key Project Grant 10533010, and Grant 10575004; by the Chinese Academy of Sciences under grant KJCX3-SYW-N2; and by the Ministry of Science and Technology under the National Basic Sciences Program (973) under grant 2007CB815401. A.R.L. thanks the Institute for Astronomy, University of Hawaii, for hospitality while this work was completed. We acknowledge use of the CosmoMC package [15].

-
- [1] W. Hu and D. J. Eisenstein, Phys. Rev. D **59**, 083509 (1999), [arXiv:astro-ph/9809368](#).
 - [2] I. Wasserman, Phys. Rev. D **66**, 123511 (2002), [arXiv:astro-ph/0203137](#).
 - [3] C. Rubano and P. Scudellaro, Gen. Rel. and Grav. **34**, 1931 (2002), [arXiv:astro-ph/0203225](#).
 - [4] M. Kunz, [arXiv:astro-ph/0702615](#).
 - [5] M. Kunz and D. Sapone, Phys. Rev. Lett. **98**, 121301 (2007), [arXiv:astro-ph/0612452](#); W. Hu, [arXiv:0906.2024](#) [[astro-ph](#)].
 - [6] E. Komatsu *et al.*, Astrophys. J. Suppl. **180**, 330 (2009), [arXiv:0803.0547](#) [[astro-ph](#)].
 - [7] A. Chevallier and D. Polarski, Int. J. Mod. Phys. D **10**, 213 (2001), [arXiv:gr-qc/0009008](#); E. V. Linder, Phys. Rev. D **68**, 083504 (2003), [arXiv:astro-ph/0304001](#).
 - [8] B. A. Bassett, P. S. Corasaniti and M. Kunz, Astrophys. J. **617**, L1 (2004), [arXiv:astro-ph/0407364](#).
 - [9] A. G. Riess *et al.*, Astrophys. J. **699** (2009) 539 [arXiv:0905.0695](#) [[astro-ph.CO](#)].
 - [10] M. Kowalski *et al.*, Astrophys. J. **686**, 749 (2008) [arXiv:0804.4142](#) [[astro-ph](#)].
 - [11] Y. Wang and P. Mukherjee, Phys. Rev. D **76**, 103533 (2007) [arXiv:astro-ph/0703780](#).
 - [12] W. J. Percival, *et al.*, [arXiv:0907.1660](#) [[astro-ph.CO](#)].
 - [13] M. J. Mortonson, W. Hu, and D. Huterer, [arXiv:0908.1408](#) [[astro-ph](#)].
 - [14] P. S. Corasaniti, M. Kunz, D. Parkinson, E. J. Copeland, and B. A. Bassett, Phys. Rev. D **70**, 083006 (2004), [arXiv:astro-ph/0406608](#).
 - [15] A. Lewis and S. Bridle, Phys. Rev. D **66**, 103511 (2002), [arXiv:astro-ph/0205436](#).